# Finite element analysis of elastic engine bearing lubrication: theory

**Jack F. Booker* — Stephen Boedo****

** Sibley School of Mechanical and Aerospace Engineering*
*Cornell University*
*Upson Hall, Hoy Road, Ithaca*
*NY 14853 USA*

*j.f.booker@cornell.edu*

*** Department of Mechanical Engineering*
*Rochester Institute of Technology*
*76 Lomb Memorial Drive, Rochester*
*NY 14623 USA*

*sxbeme@rit.edu*

ABSTRACT. *This paper reviews the theory of finite element mode-based elastohydrodynamic lubrication analysis (as applied in a companion paper to the bearing and structural design of a dynamically loaded automotive connecting rod).*

RÉSUMÉ. *La théorie présentée de l'analyse par la méthode des éléments finis des problèmes de lubrification élastohydrodynamique exprime les déformées élastiques dans une base modale. Cet article est accompagné d'un second qui applique le modèle à l'étude des paliers de bielle de moteur d'automobile sous chargement dynamique.*

KEYWORDS: *EHL, elastohydrodynamic, lubrication, modal, analysis, bearing.*

MOTS-CLÉS : *EHL, lubrification, élastohydrodynamique, analyse, modal, palier.*

## 1. Introduction

This paper reviews the theory of finite element mode-based elastohydrodynamic lubrication (EHL) analysis (as applied in a companion paper [BOE 01] to the bearing and structural design of a dynamically loaded automotive connecting rod). As such, it does *not* attempt a general bibliographical review of the finite element method in lubrication, a task addressed elsewhere [BOU 01] in this special issue. Rather, it is limited to an outline of several decades of work by the authors and their colleagues, leading to their particular approach to problems of engine bearing lubrication analysis.

Engine bearing loading presents particular problems for lubrication analysis. The relatively high magnitude of loading introduces significant elastic deformation, while the rapid variation of loading makes conservation of mass in cavitated films a necessary analysis feature. Both features can be accommodated quite naturally via finite element analysis, bringing also the usual advantages of irregular meshes for irregular geometries. Modal analysis further allows a lower-order representation of structural displacement patterns, resulting in a robust and efficient simulation procedure which accommodates unrelated meshes for fluid and solid surfaces; as an additional potential benefit, modal interpretation of dynamic behavior may be of use in guiding structural design modifications [BOE 97b].

While engine bearing analyses typically concern *cylindrical* geometries, the methods described here have equally well been applied to *planar* [BOE 95a] and *spherical* geometries [KOT 95].

Presentation takes the form of a series of major sections covering related topics. Topics are introduced in 'bottom-up' order, starting with basic (distributed) relations of fluid and solid mechanics, followed by discretization via finite element analysis. Next, fluid/solid interaction (coupling) relations are introduced in discrete form, leading then to a discrete initial-boundary-value problem with algebraic constraints. Finally, this 'nodal' problem is replaced by a similar lower-order 'modal' problem through introduction of a constraining transformation to generalized coordinates.

The authors have elected an unusual mode of presentation, whereby each set of relations is presented *en bloc*, followed by an explanatory commentary.

## 2. Fluid

### 2.1. *Mechanics*

#### 2.1.1. *Mean motion: momentum & constitution*

$$\langle \mathbf{u} \rangle = \underbrace{\langle \mathbf{u}^{a,b} \rangle}_{\textit{Couette}} - \underbrace{(1/12)(h^2/\mu)\, \nabla p}_{\textit{Poiseuille}} \qquad [1]$$

with

$$\langle \mathbf{u}^{a,b} \rangle \equiv (\mathbf{u}^a + \mathbf{u}^b)/2 \qquad [2]$$

2.1.2. *Power dissipation*

$$H = H_{Couette} + H_{Poiseuille} \geq 0 \qquad [3]$$

with

$$H_{Couette} \equiv \int_A (\mu/h)\, \Delta\mathbf{u} \cdot \Delta\mathbf{u}\, dA \qquad \geq 0 \qquad [4]$$

$$H_{Poiseuille} \equiv \int_A (1/12)(h^3/\mu)\, \nabla p \cdot \nabla p \;\; dA \;\; \geq 0 \qquad [5]$$

with

$$\Delta\mathbf{u} \equiv \;\; \mathbf{u}^b - \mathbf{u}^a \qquad [6]$$

2.1.3. *Surface tractions*

$$\tau^a = -\,(\mu\,/h)\,\Delta u + \nabla(ph/2) - p\,\nabla\langle z\rangle \qquad [7]$$

$$\tau^b = +\,(\mu\,/h)\,\Delta u + \nabla(ph/2) + p\,\nabla\langle z\rangle \qquad [8]$$

with mean surface position[1]

$$\langle z\rangle \equiv (z^a + z^b)/2 \qquad [9]$$

so

$$\boldsymbol{\tau^a + \tau^b = \nabla(ph)} \qquad [10]$$

2.1.4. *Areal density: definition*

$$\rho^* \equiv \rho h \qquad [11]$$

2.1.5. *Lineal flux: definition*

$$\boldsymbol{f} \equiv \rho h \langle \mathbf{u} \rangle \equiv \rho^* \langle \mathbf{u} \rangle \qquad [12]$$

1. Mean surface position is everywhere zero for a mid-film coordinate system [BOO 89].

2.1.6. *Continuity: mass conservation*

$$\int_S \mathbf{n} \cdot \boldsymbol{f} \, dS + \left( \int_A \rho^* \, dA \right)_{,t} = 0 \qquad [13]$$

2.1.7. *Commentary*

Figure 1 shows solid bearing surfaces 'a' and 'b' separated by a fluid film of thickness h.

Figure 2 shows an *arbitrary* cylindrical section of fluid film, its projection onto the x-y reference plane, and 2-D mass flux and normal vectors on its boundary.

Figure 3 again shows the 2-D quantities in the x-y plane.

Detailed derivations of relations [1-13] are available elsewhere [BOO 89]. All vector quantities therein are 2-D, lying in the x-y reference plane.

Derivation of mean fluid velocity relation [1] reflects equilibrated flow of a purely viscous (inertialess) fluid between impervious surfaces without slip. Though the full derivation is complex, all but the constant value can be inferred by dimensional analysis considerations. Such purely viscous 'creeping' flows consist only of surface ('Couette') and pressure gradient ('Poiseuille') driven components, as seen in both the equation of motion [1] and the power dissipation relations [3-5].

Surface tractions [7,8] act *on* fluid surfaces 'a' and 'b' as indicated.

Relatively unfamiliar *areal* (as contrasted with *volumetric*) mass density [11] and *lineal* (as opposed to *areal*) mass flux [12] are appropriate for thin film analysis.

Mass conservation relation [13] implies impervious surfaces 'a' and 'b' .

## 2.2. *Mathematical forms*

2.2.1. *Continuity: integral (weak) form*

$$\int_A \left( \nabla \cdot \boldsymbol{f} + \rho^*_{,t} \right) dA = 0 \qquad [14]$$

2.2.2. *Continuity: differential (strong) form*

$$\nabla \cdot \boldsymbol{f} + \rho^*_{,t} = 0 \qquad [15]$$

2.2.3. *Continuity: integral (weighted) form*

$$\int_A \phi \left( \nabla \cdot \boldsymbol{f} + \rho^*_{,t} \right) dA = 0 \qquad [16]$$

2.2.4. *Combination: continuity & motion (Reynolds equation)*

$$\nabla \cdot (h^2/12)(\rho^*/\mu)\nabla p = \rho^*_{,t} + \nabla \cdot \rho^* < \mathbf{u}^{a,b} >$$

*diffusion* *unsteady* *steady (convection/entrainment)*

$$= \rho^*_{,t} + \nabla\rho^* \cdot < u^{a,b} > + \rho^* \nabla \cdot < u^{a,b} > \qquad [17]$$

*squeeze* *wedge* *stretch*

or

$$\nabla \cdot (h^3/12)(\rho/\mu)\nabla p = (\rho h)_{,t} + \nabla \cdot (\rho h) < \mathbf{u}^{a,b} >$$

$$= \rho h_{,t} + h\rho_{,t} \qquad \textit{squeeze}$$

$$+ \rho \nabla h \cdot < \mathbf{u}^{a,b} > + h \nabla\rho \cdot < \mathbf{u}^{a,b} > \qquad \textit{wedge}$$

$$+ \rho h \nabla \cdot < \mathbf{u}^{a,b} > \qquad \textit{stretch} \quad [18]$$

2.2.5. *Functional (augumented)*

$$J = 1/2 \int_A (h^2/12)(\rho^*/\mu)\nabla p \cdot \nabla p \, dA$$

$$- \int_A \rho^* < \mathbf{u}^{a,b} > \cdot \nabla p \, dA + \int_A \rho^*_{,t} \, p \, dA$$

$$+ \int_{Sf} \boldsymbol{f} \cdot \mathbf{n} \, p \, dS \qquad [19]$$

2.2.6. *Commentary*

Continuity forms [14-16] evidently derive directly from [13] through application of the divergence theorem, noting that the region of integration is *arbitrary*.

The Reynolds equation is of such great importance in lubrication analysis that alternate forms [17,18] are shown and their terms appropriately identified. (It should be noted that the labeled 'stretch' term is negligible for ordinary bearings.)

The augmented functional [19] corresponding to [17] is a common starting point for approximate solutions.

### 2.3. *Distributed problem formulation*

2.3.1. *Boundary conditions*

boundary $S_p$ : $p$ *'essential'* [20]

boundary $S_f$ : $\boldsymbol{f} \cdot \mathbf{n}$ *'natural'* [21]

with

$$S = S_p \cup S_f \qquad [22]$$

where $S_p$ is non-vanishing.

2.3.2. *Boundary-value problem*

Satisfy combined field equation [17/18] with respect to pressure distribution p meeting *both* conditions [20] and [21].

2.3.3. *Variational problem*

Minimize augmented functional [19] with respect to pressure distribution p meeting *only* condition [20], thus meeting condition [21] *naturally*.

(The two problem formulations are formally equivalent [BOO 72].)

### 2.4. *Discrete relations*

2.4.1. *Variational method*

$$J = 1/2 \int_A (h^2/12)\,(\rho^*/\mu)\,\nabla p \cdot \nabla p\, dA$$

$$- \int_A \rho^* < \mathbf{u}^{a,b} > \cdot \nabla p\, dA + \int_A \rho^*_{,t}\, p\, dA$$

$$+ \int_{Sf} \boldsymbol{f} \cdot \mathbf{n}\, p\, dS \qquad [19]$$

with

$$p = \Sigma\, N_i\, p_i \qquad [23]$$

gives

$$J = 1/2\, \Sigma\Sigma\, p_i\, F_{ij}\, p_j - \Sigma\, q_i\, p_i - \Sigma\, q^e{}_i\, p_i \qquad [24]$$

so

$$\partial J/\partial p_i = 0$$

gives

$$\Sigma F_{ij}\, p_j = q_i + q^e{}_i \qquad [25]$$

with

$$F_{ij} \equiv \int_A (h^2/12)\,(\rho^*/\mu)\,\nabla N_i \cdot \nabla N_j\, dA \qquad [26]$$

$$q_i \equiv - \int_{Sf} \boldsymbol{f} \cdot \mathbf{n}\, N_i\, dA \qquad [27]$$

$$q^e{}_i = q^u{}_i + q^{\partial\rho^*}{}_i \qquad [28]$$

with

$$q^{u}_{i} \equiv \int_A \rho^* < \mathbf{u}^{a,b}> \cdot \nabla N_i \, dA \qquad [29]$$

$$q^{\partial\rho^*}_{i} \equiv - \int_A \rho^*_{,t} \, N_i \, dA \qquad [30]$$

2.4.2. Weighted residual (Galerkin) method

$$\int_A \phi \, ( \nabla \cdot \boldsymbol{f} + \rho^*_{,t} ) \, dA = 0 \qquad [16]$$

with

$$p = \Sigma N_i \, p_i \qquad [23]$$

$$\phi = \Sigma N_i \, \phi_i \qquad [31]$$

gives essentially the same result [24-29].

2.4.3. *Alternate forms*

$$F_{ij} \equiv \int_A (h^3/12) \, (\rho/\mu) \, (N_{i,x} \, N_{j,x} + N_{i,y} \, N_{j,y}) \, Da \qquad [32]$$

$$q^{e}_{i} = q^{ux}_{i} + q^{uy}_{i} + q^{\partial h}_{i} + q^{\partial\rho}_{i} \qquad [33]$$

with

$$q^{ux}_{i} \equiv \int_A \rho h < u^{xa,b}> N_{i,x} \, dA \qquad [34]$$

$$q^{uy}_{i} \equiv \int_A \rho h < u^{ya,b}> N_{i,y} \, dA \qquad [35]$$

$$q^{\partial h}_{i} \equiv - \int_A \rho \, h_{,t} \, N_i \, dA \qquad [36]$$

$$q^{\partial\rho}_{i} \equiv - \int_A h \, \rho_{,t} \, N_i \, dA \qquad [37]$$

so if

$$\rho_{,t} = \Sigma N_j \, D\rho_j \qquad [38]$$

$$h_{,t} = \Sigma N_j \, Dh_j \qquad [39]$$

$$< u^{xa,b}> = \Sigma N_j < u^{xa,b}>_j \qquad [40]$$

$$< u^{ya,b}> = \Sigma N_j < u^{ya,b}>_j \qquad [41]$$

then

$$q^{ux}_{i} \equiv (\Sigma \int_A \rho h \, N_{i,x} \, N_j \, dA) < u^{xa,b}>_j \equiv Q^{ux}_{ij} < u^{xa,b}>_j \qquad [42]$$

$$q^{uy}_{i} \equiv (\Sigma \int_A \rho h \, N_{i,y} \, N_j \, dA) < u^{ya,b}>_j \equiv Q^{uy}_{ij} < u^{ya,b}>_j \qquad [43]$$

$$q^{\partial h}_i \equiv -(\Sigma \int_A \rho\, N_i\, N_j\, dA)\, Dh_j \equiv Q^{Dh}_{ij}\, Dh_j \qquad [44]$$

$$q^{\partial \rho}_i \equiv -(\Sigma \int_A h\, N_i\, N_j\, dA)\, D\rho_j \equiv Q^{D\rho}_{ij}\, D\rho_j \qquad [45]$$

with

$$Q^{ux}_{ij} \equiv \int_A \rho h\, N_{i,x}\, N_j\, dA \qquad [46]$$

$$Q^{uy}_{ij} \equiv \int_A \rho h\, N_{i,y}\, N_j\, dA \qquad [47]$$

$$Q^{Dh}_{ij} \equiv -\int_A \rho\, N_i N_j\, dA \qquad [48]$$

$$Q^{D\rho}_{ij} \equiv -\int_A h\, N_i N_j\, dA \qquad [49]$$

2.4.4. *Commentary*

Nodal flows $q_i$ and $q^e_i$ are here defined by [27-30] as positive *inward* (in direct opposition to the commonly applied lubrication convention [BOO 72]), thus ensuring that fluidity matrix $F_{ij}$ is here *positive* semidefinite (and singular). This break with tradition has the effect of bringing the form of lubrication equations into alignment with analogous ones from other fields (e.g., conductive heat transfer).

Interpolations [23, 38-41] require shape functions for specific elements. Appendix A.1 provides a family of such functions for the commonly-used 3-node linear triangular elements suggested by Figure 4.

Further detail requires specification of the behavior of functions h, $\rho$, $\mu$ . Appendix A.2 provides resulting matrices for these 3-node linear triangular elements with linearly interpolated h and uniform $\rho$, $\mu$ .

## 2.5. *Discrete problem formulation*

2.5.1. *Pressure-flow relation*

Supposing full knowledge of fluidity matrix $F_{ij}$ and equivalent flows $q^e_i$ , a typical problem consists of n relations

$$\Sigma F_{ij}\, p_j = q_i + q^e_i \qquad [25]$$

with n complementary knowns/unknowns $p_i$ , $q_i$ .

Since *either* pressure $p_i$ *or* flow $q_i$ (but not both) is known for each node, solution follows standard methods of finite element analysis for 'mixed' problems.

For example, pressure $p_i$ is typically known for external boundary nodes, while flow $q_i$ is typically known (zero) for internal nodes.

*Positive* values of flows $q_i$ and $q^e_i$ inspire *positive* shifts in pressure $p_i$ .

2.5.2. *Work-equivalent nodal forces*

Similarly

$$\int_A p h_{,t}\, dA = \Sigma\, r_i\, Dh_i \qquad [50]$$

with

$$= \Sigma\, N_j\, p_j \qquad [51]$$

$$h_{,t} = \Sigma\, N_i\, Dh_i \qquad [52]$$

gives

$$\Sigma A_{ij}\, p_j = r_i \qquad [53]$$

with

$$A_{ij} \equiv \int_A N_i\, N_j\, dA \qquad [54]$$

2.5.3. *Nodal kinematics*

$$d_i \equiv h_i - c_i \qquad [55]$$

2.5.4. *Nodal equation of motion*

$$\Sigma\, C_{ij}\, Dd_j + b_i = -\, r_i \qquad [56]$$

Commentary

Explicit expressions for damping $C_{ij}$ and static force $b_i$ can be obtained (with some effort) through combining relations [25], [33], [42-45], [53], [55], [56] with specified nodal $q_i$ , $p_i$ .

(As seen below, symbolic evaluation of these coefficients is not always required.)

## 2.6. *Cavitation*

2.6.1. *Mechanics*

2.6.1.1. Dynamic (mass-conserving)

$$(p - p_{cav})\,(\rho_{liq} - \rho) = 0$$

$$p_{cav} \le p$$

$$0 \le \rho \le \rho_{liq}$$

$$\mu / \mu_{liq} = \rho / \rho_{liq} \qquad [57]$$

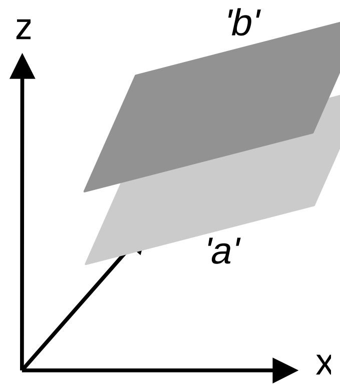


**Figure 1.** *Bearing surfaces separated by a fluid film*

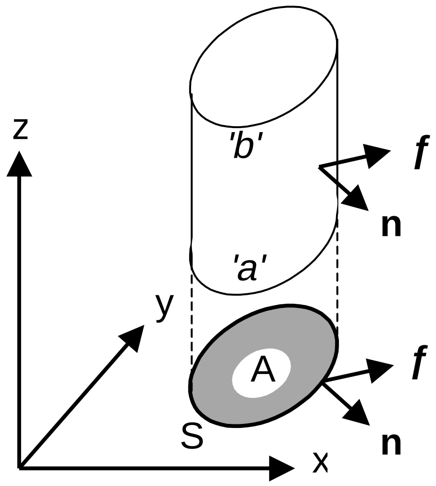


**Figure 2.** *Arbitrary cylindrical section of the film*

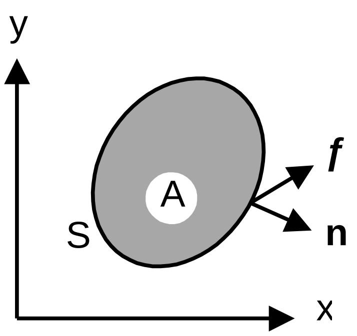


**Figure 3.** *2D projection of the cylindrical section*

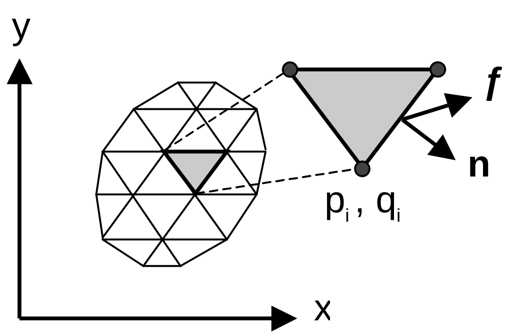


**Figure 4.** *Triangular element mesh*

2.6.1.2. Quasi-static

$$\rho = \rho_{liq}$$

$$p_{cav} \leq p$$

$$0 \leq \rho_{liq}$$

$$\mu = \mu_{liq} \qquad [58]$$

2.6.1.3. Commentary

The distributed and discrete fluid models above can be extended to address cavitation through treating the fluid film as a *mixture* of incompressible liquid and fully compressible vapor (of negligible density and viscosity). The liquid/vapor demarcation is assumed to be 2-dimensional.

Figure 5(a) illustrates the abrupt (non-analytic) pressure-density relations [57] assumed for the fluid mixture, while Figure 5(b) illustrates reduced relations [58] for a pure liquid.

2.6.2. *Problem formulation*

The distributed boundary-value problem given above is simply augmented by initial specification of mixture density to form an *initial*-boundary-value problem.

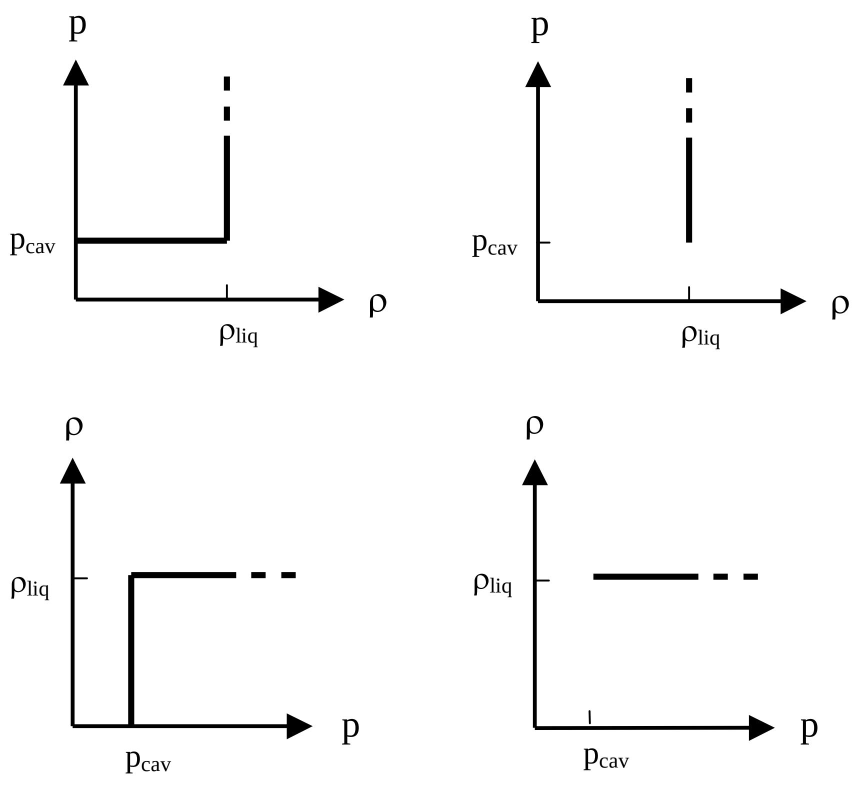


**(a)** *dynamic* **(b)** *quasi-static*

**Figure 5 (a et b).** *Mixture pressure-density relation*

2.6.3. Problem solution

The presumed scenario of cavitation under this mixture model is 3-fold:

***Initiation*** occurs instantaneously when pressure drops locally to its cavitation value, whereupon mixture density *begins* to drop from liquid value as vapor *begins* to form.

***Evolution*** of cavitation, once initiated, proceeds temporally at cavitation pressure and declining and/or increasing mixture density. (Transport in fixed-pressure cavitated zones is driven entirely by the 'Couette' term of equation [1].)

***Reformation*** occurs instantaneously wherever mixture density rises to liquid value, whereupon pressure is no longer fixed at cavitation pressure.

Discrete cavitation algorithms can be built upon quasi-static relation [25] when initial values of mixture density $\rho_i$ at internal nodes are specified initially and then integrated forward over time ([KUM 90b], [KUM 91a,b,c], [LAB 85], [BOE 95a][2], etc.)

At any one node, 1 of 3 variables (pressure $p_i$, flow $q_i$, equivalent flow $q^{\dot{\rho}}_i$) is always unknown (though iteration may be necessary to determine *which* one). For example, suppose that the fluid film is initially entirely liquid and that boundary nodes have fixed pressure (greater than cavitation value) and null density rate flow; for boundary nodes the unknown variable is flow. At any one interior node flow is null, pressure is greater than/equal to cavitation value, and density rate equivalent flow is greater than/equal to zero; iteration with quasi-static relation [25] determines a consistent pairing of nodal pressure and density rate equivalent flow. (Nodal density rate is then determined from density rate equivalent flow.)

If nodal density rates are used to integrate nodal density values forward in time, the resulting "*dynamic*" algorithm is mass-conserving; if nodal density is maintained at its liquid value, the resulting *'quasi-static'* algorithm is *not* mass-conserving.

## 3. Solid

### *Discrete relations*

Structural solids follow the conventional relations of quasi-static linear elasticity embodied in commercial software and expressed in discretized form as

$$\Sigma K_{ij}\, d_j = r_i + r^e_i \qquad [59]$$

2. Such "normal separation" studies are much more general than may be supposed, since the (arbitrary) x-y reference frame can always be chosen in such a way that *observed* mean tangential surface motion vanishes.

where equivalent nodal forces $r^e_i$ encompass external load, body forces, etc. Because displacements $d_i$ are *relative*, stiffness $K_{ij}$ and forces $r_i$ must be derived from their more conventional counterparts (based on *absolute* displacements); detailed formulas for such derivations are available [KUM 90, BOE 97a, BOE 00]. It should be noted that stiffness matrix $K_{ij}$ is always singular, since *rigid body* relative displacements $d_i$ must be allowed.

## 4. Fluid-solid system

### 4.1. *Discrete relations*

4.1.1. *Fluid*

$$\underline{\underline{\mathbf{C}}}(\underline{\mathbf{d}},t)\, D\underline{\mathbf{d}} + \underline{\mathbf{b}}(\underline{\mathbf{d}},t) = -\,\underline{\mathbf{r}}(t) \qquad [56]$$

4.1.2. *Solid*

$$\underline{\underline{\mathbf{K}}}\,\underline{\mathbf{d}} = \underline{\mathbf{r}} + \underline{\mathbf{r}}^e \qquad [59]$$

4.1.3. *Commentary*

Singly subscripted variables are represented by singly underlined bold symbols, and doubly subscripted variables are represented by doubly underlined bold symbols.

– Vector $\underline{\mathbf{c}}$ and matrices $\underline{\underline{\mathbf{A}}}$ and $\underline{\underline{\mathbf{K}}}$ are considered fixed system parameters.

– Vector $\underline{\mathbf{b}}$ and matrix $\underline{\underline{\mathbf{C}}}$ are known functions of $\underline{\mathbf{d}}$ (and t).

– Vector $\underline{\mathbf{b}}$ and matrix $\underline{\underline{\mathbf{C}}}$ depend on matrices $\underline{\underline{\mathbf{A}}}$ , $\underline{\underline{\mathbf{F}}}$ , and $\underline{\underline{\mathbf{Q}}}^e$.

– Vector $\underline{\mathbf{r}}^e$ is a known function of t.

– Matrices $\underline{\underline{\mathbf{A}}}$ , $\underline{\underline{\mathbf{K}}}$ , and $\underline{\underline{\mathbf{C}}}$ are square and symmetric (iffi $\rho$ is uniform).

– Matrix $\underline{\underline{\mathbf{A}}}$ is nonsingular, while both $\underline{\underline{\mathbf{K}}}$ and $\underline{\underline{\mathbf{C}}}$ are singular.

Relations [56], [59] appear variously [KUM 89,90], [KOT 95], [BOE 97a,b], etc. (These relations can be considered generalizations of other relations developed for a very simple prototypical application [BOO 84].)

### 4.2. *Modal problem*

4.2.1. *Kinematic constraint transformation*

$$\underline{\mathbf{d}} = \underline{\underline{\mathbf{T}}}\,\underline{\mathbf{d}}' \qquad [60]$$

4.2.2. *Constrained solid*

$$\underline{\underline{\mathbf{K}}}'\,\underline{\mathbf{d}}' = \underline{\mathbf{r}}' + \underline{\mathbf{r}}^{e\,\prime} \qquad [61]$$

where

$$\underline{\underline{\mathbf{K}}}' \equiv \underline{\underline{\mathbf{T}}}^{T}\,\underline{\underline{\mathbf{K}}}\,\underline{\underline{\mathbf{T}}} \qquad [62]$$

$$\underline{\mathbf{r}}' \equiv \underline{\underline{\mathbf{T}}}^{T}\,\underline{\mathbf{r}} \qquad [63]$$

$$\underline{\mathbf{r}}^{e\,\prime} \equiv \underline{\underline{\mathbf{T}}}^{T}\,\underline{\mathbf{r}}^{e} \qquad [64]$$

4.2.3. *Constrained fluid*

$$\underline{\underline{\mathbf{C}}}'(\underline{\mathbf{d}}',t)\,\mathrm{D}\underline{\mathbf{d}}' + \underline{\mathbf{b}}'(\underline{\mathbf{d}}',t) = -\,\underline{\mathbf{r}}'(t) \qquad [65]$$

where

$$\underline{\underline{\mathbf{C}}}' \equiv \underline{\underline{\mathbf{T}}}^{T}\,\underline{\underline{\mathbf{C}}}\,\underline{\underline{\mathbf{T}}} \qquad [66]$$

$$\underline{\mathbf{b}}' \equiv \underline{\underline{\mathbf{T}}}^{T}\,\underline{\mathbf{b}} \qquad [67]$$

$$\underline{\mathbf{r}}' \equiv \underline{\underline{\mathbf{T}}}^{T}\,\underline{\mathbf{r}} \qquad [63]$$

4.2.4. *Constrained fluid-solid system*

$$\underline{\underline{\mathbf{C}}}'(\underline{\mathbf{d}}',t)\,\mathrm{D}\underline{\mathbf{d}}' + \underline{\mathbf{b}}'(\underline{\mathbf{d}}',t) + \underline{\underline{\mathbf{K}}}'\,\underline{\mathbf{d}}' = \underline{\mathbf{r}}^{e\,\prime}(t) \qquad [68]$$

or

$$\mathrm{D}\underline{\mathbf{d}}' = \underline{\underline{\mathbf{C}}}'^{\,-1}\left(\underline{\mathbf{r}}^{e\,\prime} - \underline{\mathbf{b}}' - \underline{\underline{\mathbf{K}}}'\,\underline{\mathbf{d}}'\right) \qquad [69]$$

4.2.5. *Commentary*

Due account is taken of forces of constraint in forming the transformations.

The chief motivation for the transformations is reduction in system order. Owing to the (normally radically) reduced order of the modal representation, *numerical* determination of the coefficients $\underline{\underline{\mathbf{C}}}'$ and $\underline{\mathbf{b}}'$ via [56] is conventional. However, additional advantages accrue. For example, generalized coordinates $\mathbf{d}'$ may themselves be more intuitively meaningful than nodal displacements $\mathbf{d}$ .

In principle, transformation $\underline{\underline{\mathbf{T}}}$ could be selected in a wide variety of ways. Discrete (nodal) versions of distributed orthogonal functions would be attractive, allowing quite seamlessly for unrelated separate meshes on fluid and solid surfaces. On the other hand, if $\underline{\underline{\mathbf{T}}}$ satisfies the general eigenproblem [BOE 95b]

$$\underline{\underline{\mathbf{T}}}^{T}\,\underline{\underline{\mathbf{K}}}\,\underline{\underline{\mathbf{T}}} = \underline{\underline{\mathbf{T}}}^{T}\,\underline{\underline{\mathbf{A}}}\,\underline{\underline{\mathbf{T}}}\ \ \underline{\underline{\Delta}} \qquad [70]$$

where matrix $\underline{\underline{\Delta}}$ is a diagonal "spectral" matrix of (unknown) eigenvalues, then $\underline{\underline{\mathbf{K}}}'$ and $\underline{\underline{\mathbf{A}}}'$ are diagonal, and the resulting transformation $\underline{\underline{\mathbf{T}}}$ is mesh-invariant (in the sense that the basic *shape* of modes is invariant). This common approach also allows relatively easily for unrelated separate meshes on fluid and solid surfaces following a *single* (static) translation of $\underline{\underline{\mathbf{T}}}$ from solid to fluid mesh representation. An example of a transformation mode family obtained in this fashion is illustrated in the companion paper [BOE 01]. There the eigenmode shapes are shown in order of their corresponding eigenvalues, progressing from rigid body modeshapes (corresponding to null eigenvalues) to successively more complex elastic modes, usually (though not always) occurring in rough pairs. (It can be shown formally that the ordering of suitably normalized eigenmode shapes by modal strain energy is equivalent to ordering by their eigenvalues.)

No matter how the transformation mode family may finally be calculated, a judicious *selection* from it is necessary to obtain desired reduction in system order. As demonstrated in the companion paper [BOE 01], the selection process can be approached iteratively, adding higher modes until apparent numerical convergence. Fortunately, the section process need only be performed once for a particular design.

(If only rigid body modes are selected, analysis reduces to one for rigid surfaces.)

Whatever modes are selected, modal displacements (generalized coordinates) contained in $\underline{\mathbf{d}}'$ are specified initially and then numerically integrated forward in time according to the system ODE [69]. In the event that dynamic cavitation is to be considered, fluid mixture density ρ must be followed in time as well.

See [KUM 89], [KUM 90a], [BOE 95b], [BOE 97a] for details of this modal formulation and [OLS 97], [OLS 01] for details of a variation not covered here.

## 5. Nomenclature

### 5.1. *Distributed variables*

| | | |
|---|---|---|
| t | time | [T] |
| x,y,z | spatial coordinates | [L] |
| D | temporal derivative (total) | $[T^{-1}]$ |
| ,t | temporal derivative (partial) | $[T^{-1}]$ |
| ∇ | spatial derivative | $[L^{-1}]$ |
| A | area | $[L^2]$ |
| S | boundary | [L] |
| **n** | unit outward normal | [–] |
| h | thickness | [L] |
| c | clearance | [L] |
| d | displacement | [L] |
| μ | viscosity | $[FL^{-2}T]$ |
| ρ | volumetric mass density | $[ML^{-3}]$ |
| ρ* | areal mass density | $[ML^{-2}]$ |
| ***f*** | lineal mass flux | $[ML^{-1}T^{-1}]$ |
| **u** | fluid velocity | $[LT^{-1}]$ |

| | | |
|---|---|---|
| $\mathbf{u}^a$, $\mathbf{u}^b$ | surface velocities | $[LT^{-1}]$ |
| $\langle z \rangle$ | surface position average | [L] |
| $\langle \mathbf{u} \rangle$ | fluid velocity average | $[LT^{-1}]$ |
| $\langle \mathbf{u}^{a,b} \rangle$ | surface velocity average | $[LT^{-1}]$ |
| $\Delta\mathbf{u}$ | surface velocity difference | $[LT^{-1}]$ |
| p | pressure | $[FL^{-2}]$ |
| $\tau$ | surface traction | $[FL^{-2}]$ |
| J | functional | $[F^2L^{-3}T]$ |
| H | power dissipation | $[FLT^{-1}]$ |
| $\phi$ | weight function | [–] |
| $N_i$ | shape function | [–] |

### 5.2. *Discrete variables*

| | | |
|---|---|---|
| i, j, k | node index | [–] |
| n | node total | [–] |
| $F_{ij}$ | fluidity | [LT] |
| $Q_{ij}$ | fluidity | [various] |
| $q_i$ | flow | $[MT^{-1}]$ |
| $q^e{}_i$ | equivalent flow | $[MT^{-1}]$ |
| $C_{ij}$ | damping | $[FL^{-1} T]$ |
| $K_{ij}$ | stiffness | $[FL^{-1}]$ |
| $b_i$ | static force | [F] |
| $r_i$ | force | [F] |
| $r^e{}_i$ | equivalent force | [F] |
| $T_{ij}$ | transformation | [L][3] |
| $\Lambda_{ii}$ | eigenvalue | $[FL^{-3}]$ |

## 6. References

[BOE 95a] BOEDO S., BOOKER J.F., “Cavitation in normal separation of square and circular plates”, *ASME Journal of Tribology*, vol. 117 no. 3, 1995, pp. 403-410.

[BOE 95b] BOEDO S., BOOKER J.F., WILKIE M.J., “A mass conserving modal analysis for elastohydrodynamic lubrication”, *Proc. 21st Leeds-Lyon Symposium on Tribology*: Lubricants and Lubrication, 1995, Elsevier, pp. 513-523.

3. Dimensions shown correspond to case of *dimensionless* modal displacements (generalized coordinates).

[BOE 95c] BOEDO S., BOOKER J.F., "Body force and surface roughness effects in a mass-conserving mode-based elastohydrodynamic lubrication model", *Proc. Japan International Tribology Conference*, 1995.

[BOE 97a] BOEDO S., BOOKER J.F., "Surface roughness and structural inertia in a mode-based mass-conserving elastohydrodynamic lubrication model", *ASME Journal of Tribology*, vol. 119 no. 3, 1997, pp. 449-455.

[BOE 97b] BOEDO S., BOOKER J.F., "Mode stiffness variation in elastohydrodynamic bearing design", *Proc. 23rd Leeds-Lyon Symposium on Tribology: Elastohydrodynamics - Fundamentals and Applications of Lubrication and Traction*, 1997, Elsevier, pp. 685-697, 740-741.

[BOE 00] BOEDO S., BOOKER J.F., "A mode-based elastohydrodynamic lubrication model with elastic journal and sleeve", *ASME Journal of Tribology*, vol. 122 no. 1, 2000, pp. 94-102.

[BOE 01] BOEDO S., BOOKER J.F., "Finite element analysis of elastic engine bearing lubrication: Application", *Revue européenne des eléments finis*, vol. 10 no.7-8, 2001.

[BOO 72] BOOKER J.F., HUEBNER K.H., "Application of finite-element methods to lubrication: an engineering approach", ASME Journal of Lubrication Technology, vol. 94 no. 4, 1972, p. 313-323. Errata: Vol. 98, No. 1, January 1976, p. 39.

[BOO 84] BOOKER J.F., SHU C.F., "Finite element analysis of transient elasto-hydrodynamic lubrication", *Proc. 10th Leeds-Lyon Symposium on Tribology:Developments in Numerical and Experimental Methods Applied to Tribology*, 1984, Butterworths, p. 157-163.

[BOO 89] BOOKER J.F., "Basic equations for fluid films with variable properties", *ASME Journal of Tribology*, vol. 111 no. 3, 1989, pp. 475-483.

[BOU 01] BOU-SAID B., "La méthode des eléments finis en lubrification: une revue bibliographique", *Revue européenne des eléments finis*, vol. 10, no. 7-8, 2001.

[EID 76] EIDELBERG B.E., BOOKER J.F., "Application of finite element methods to lubrication: squeeze films between porous surfaces", *ASME Journal of Lubrication Technology*, vol. 98 no. 1, 1976, pp. 175-180,186.

[GOE 80] GOENKA P.K., BOOKER J.F., "Spherical bearings: static and dynamic analysis via the finite element method", *ASME Journal of Lubrication Technology*, vol. 102 no. 3, 1980, pp. 308-319.

[GOE 83] GOENKA P.K., BOOKER J.F., "Effect of surface ellipticity on dynamically loaded cylindrical bearings", *ASME Journal of Lubrication Technology*, vol. 105 no. 1, 1983, p. 1-12.

[KOT 95] KOTHARI M., BOOKER J.F., BARTEL D.L., "Analysis of artificial hip joints as spherical bearings", *Proc. 21st Leeds-Lyon Symposium on Trib*ology: Lubricants and Lubrication, 1995, Elsevier, pp. 93-98.

[KUM 89] KUMAR A., BOOKER J.F., GOENKA P.K, "Dynamically loaded journal bearings: a modal approach to EHL design analysis", *Proc. 15th Leeds-Lyon Symposium on Tribology: Tribological Design of Machine Elements*, 1989, Elsevier, pp. 305-315, 508-510.

[KUM 90a] Kumar A., Goenka P.K., Booker J.F., "Modal analysis of elastohydrodynamic lubrication: a connecting rod application", *ASME Journal of Tribology*, vol. 112 no. 3, 1990, p. 524-534.

[KUM 90b] Kumar A., Booker J.F., "Cavitation and thermal effects in journal bearing applications", *Proc. Japan International Tribology Conference*, 1990, p. 1491-1496.

[KUM 91a] Kumar A., Booker J.F., "A finite element cavitation algorithm", *ASME Journal of Tribology,* vol. 113 no. 2, 1991, p. 276-286.

[KUM 91b] Kumar A., Booker J.F., "A finite element cavitation algorithm: application/validation", *ASME Journal of Tribology*, vol. 113 no. 2, 1991, p. 255-261.

[KUM 91c] Kumar A., Booker J.F., "Mass-conservative cavitation analysis for engine bearings", *Proc. 17th Leeds-Lyon Symposium on Tribology: Vehicle Tribology*, 1991, Elsevier, p. 27-32.

[KUM 94] Kumar A., Booker J.F., "A mass and energy conserving finite element lubrication algorithm", *ASME Journal of Tribology*, vol. 116 no. 4,1994, p. 667-671.

[LAB 85] LABOUFF G.A., BOOKER J.F., "Dynamically loaded journal bearings: a finite element treatment for rigid and elastic surfaces", *ASME Journal of Tribology*, vol. 107 no. 4, 1985, pp. 505-515.

[OLS 97] OLSON E.G., BOOKER J.F., "A finite element treatment of hydrodynamically lubricated journal bearings with structural inertia and elasticity", *Proc. 23rd Leeds-Lyon Symposium on Tribology: Elastohydrodynamics - Fundamentals and Applications of Lubrication and Traction,* 1997, Elsevier, p. 661-673.

[OLS 01] OLSON E.G., BOOKER J.F., "EHD Analysis with Distributed Structural Inertia", *ASME Journal of Tribology*, vol. 123 no. 3, 2001, p. 462-468.

## Appendix A. 3-node triangular element

*Reference:* [BOO 72]

### A.1. *Shape functions*

A typical element has 3 nodes numbered (consecutively) counterclockwise and 3 linear shape (interpolation) functions

$$N_i(x,y) = (a_i + b_i x + c_i y) / (2A) \quad [A1]$$

orthonormalized such that

$$N_i(x_j, y_j) = \delta_{ij} \quad [A2]$$

so that more generally

$$\Sigma N_i(x,y) = 1 \quad [A3]$$

Setting (arbitrarily)

$$2A = a_1 + a_2 + a_3 \qquad [A4]$$

the required coefficients are thus

$$a_1 = x_2y_3 - x_3y_2 \qquad b_1 = y_2 - y_3 \qquad c_1 = x_3 - x_2$$
$$a_2 = x_3y_1 - x_1y_3 \qquad b_2 = y_3 - y_1 \qquad c_2 = x_1 - x_3$$
$$a_3 = x_1y_2 - x_2y_1 \qquad b_3 = y_1 - y_2 \qquad c_3 = x_2 - x_1 \qquad [A5]$$

Differentiation gives

$$N_{i},_{x} = b_i / (2A)$$
$$N_{i},_{y} = c_i / (2A) \qquad [A6]$$

while integration gives

$$< N_1^{l} N_2^{m} N_3^{n} > \equiv (1/A) \int N_1^{l} N_2^{m} N_3^{n} \, dA = 2 \, l! \, m! \, n! \, / \, (2+l+m+n)! \qquad [A7]$$

## A.2. *Fluid matrices*

If

$$h = \Sigma \, N_j \, h_j \qquad [A8]$$

$$\rho \, , \, \mu = \text{uniform} \qquad [A9]$$

then

$$A_{ij} = (1+ \delta_{ij}) \, A /12 \qquad [A10]$$

$$F_{ij} = (\rho/\mu) < h^3 > (b_i \, b_j + c_i \, c_j) / (48A) \qquad [A11]$$

$$Q^{ux}{}_{ij} = \rho \, b_i \, f_j / 24 \qquad [A12]$$

$$Q^{uy}{}_{ij} = \rho \, c_i \, f_j / 24 \qquad [A13]$$

$$Q^{Dh}{}_{ij} = - \, \rho \, (1+ \delta_{ij}) \, A /12 \qquad [A14]$$

$$Q^{D\rho}{}_{ij} = - \, G_{ij} \, A /60 \qquad [A15]$$

with

$$f_j \equiv \int h_k \, (1 + \delta_{kj}) = \int h_k + h_j = 3 < h > + \, h_j \qquad [A16]$$

$$G_{ij} \equiv \int h_k \, [(1 + \delta_{ij}) + (\delta_{ik} + \delta_{kj})^2 \, ]$$

$$= 3 < h > (1 + \delta_{ij}) + 2 \int h_k \, \delta_{ik} \, \delta_{kj} + h_i + h_j \qquad [A17]$$

with

$$< h > \quad = \int h_k / 3 \qquad [A18]$$

$$< h^3 > \quad = (\int h_k \int h_k^2 + \Pi h_k) /10 \qquad [A19]$$

with indicated sums and products over

$$k = 1 \text{ to } 3 \qquad [A20]$$